The Cryosphere Discuss., 6, 89–124, 2012
www.the-cryosphere-discuss.net/6/89/2012/
doi:10.5194/tcd-6-89-2012

The Cryosphere Discussions

Numerical modeling of permafrost dynamics in Alaska using a high spatial resolution dataset

E. E. Jafarov, S. S. Marchenko, and V. E. Romanovsky

Geophysical Institute, University of Alaska Fairbanks, USA

Received: 2 December 2011 – Accepted: 5 December 2011 – Published: 6 January 2012

Correspondence to: E. E. Jafarov (eejafarov@alaska.edu)

Published by Copernicus Publications on behalf of the European Geosciences Union.

Abstract

Climate projections for the 21st century indicate that there could be a pronounced warming and permafrost degradation in the Arctic and sub-Arctic regions. Climate warming is likely to cause permafrost thawing with subsequent effects on surface albedo, hydrology, soil organic matter storage and greenhouse gas emissions. To assess possible changes in the permafrost thermal state and active layer thickness, we implemented the GIPL2-MPI transient numerical model for the entire Alaska permafrost domain. Input parameters to the model are spatial datasets of mean monthly air temperature and precipitation, prescribed thermal properties of the multilayered soil column, and water content which are specific for each soil class and geographical location. As a climate forcing we used the composite of five IPCC Global Circulation Models that has been downscaled to 2 by 2 km spatial resolution by Scenarios Network for Alaska Planning (SNAP) group.

In this paper we present the preliminary modeling results based on input of five-model composite with A1B carbon emission scenario. The model has been calibrated according to the annual borehole temperature measurements for the State of Alaska. We also performed more detailed calibration for fifteen shallow borehole stations where high quality data are available on daily basis. To validate the model performance we compared simulated active layer thicknesses with observed data from CALM active layer monitoring stations. Calibrated model was used to address possible ground temperature changes for the 21st century. The model simulation results show the widespread permafrost degradation in Alaska could begin in 2040–2099 time frame within the vast area southward from the Brooks Range except for the high altitudes of the Alaska Range and Wrangell Mountains.

TCD

6, 89–124, 2012

1 Introduction

According to State of the Climate in 2010 Report (Richter-Menge and Jeffries, 2011), the arctic cryosphere is undergoing substantial changes such as loss of sea ice and warmer ocean temperatures, melting of the Greenland Ice Sheet and glaciers as well as continuous increase of permafrost temperatures. Permafrost [1], one of the main components of the cryosphere in northern regions influences hydrological processes, energy exchanges, natural hazards and carbon budgets. The World Meteorological Organization (WMO) identifies permafrost as one of six cryospheric indicators of global climate change (Brown et al., 2008). Changes of permafrost thermal state in Alaska were reported recently by Romanovsky et al. (2010) and Smith et al. (2010). They observed an increase in permafrost temperatures by 0.5 – 3°C for the last 30 years. Thawing permafrost causes land surface changes, damaging forests, houses, and infrastructure. Widespread thawing of permafrost can have a significant impact on the State economy due to the additional repair costs of public infrastructure (Larsen et al., 2008).

Mapping of permafrost distribution, especially its thermal state remains a challenging problem due to sparsity of the observed data. Despite the fact that geophysical surveys and boreholes are the most reliable sources of information about permafrost, they are extremely costly and mostly available from relatively small areas such as oil fields and transportation corridors.

In this article we propose a method based on numerical modeling which allows us to map temporal dynamics and spatial distribution of permafrost with high spatial resolution. To simulate ground thermal regimes we implement the GIPL2-MPI numerical transient model. The GIPL2 was developed by G. Tipenko and V. Romanovsky (Tipenko et al., 2004) and first time applied for the entire Alaskian permafrost domain with 0.5° spatial resolution by Marchenko et al. (2008). In order to quantify a socio-economical

[1] Permafrost is a lithospheric material, including organic, mineral soils and ground ice, where temperatures have remained at or below 0°C for a period of at least two consecutive years

TCD
6, 89–124, 2012

impact of permafrost degradation the permafrost distribution maps with higher spatial resolution are required. In the current project we map permafrost thermal state with 2 by 2 km spatial resolution, with 410205 grid points to cover the entire Alaskan region. Due to increase in the amount of spatial grid points the computational load increases as well. To perform calculations efficiently, we developed the GIPL2-MPI version of the GIPL2 model which runs in parallel on several processors. To run the parallel model we used Arctic Region Supercomputing Center facility at University of Alaska Fairbanks.

The model's input data includes climate data, snow cover, soil thermal properties, lithological data and vegetation. The main purpose of the model is to generate a spatial dataset of permafrost distribution and ground temperature dynamics as well as the active layer thickness which will be useful in a wide range of hydrologic, ecological, climatologic, and socioeconomic assessments in Alaska.

The GIPL2-MPI is an implicit finite-difference numerical model which solves a 1-D non-linear heat equation with phase change numerically and treats the process of soil freezing/thawing in accordance with relationships between the soil unfrozen water content and temperature. Special Enthalpy formulation of the energy conservation law makes it possible to use a relatively coarse vertical resolution without loss of latent heat effects in the phase transition zone. The mathematical description section gives more detailed information on the Enthalpy method. In the methods section we outline all necessary input datasets such as initial temperatures, snow, thermal properties of multi-layered organic and mineral soils, and geothermal heat flux. The model calibration and validation section provides detailed description on the model calibration with observed monthly averaged temperatures available from shallow boreholes stations and validation of the mean annual ground temperatures from deep boreholes as well as validation of the active layer thickness values with CALM [2] active layer observation stations in Alaska. The sensitivity analysis illustrates the effect of the additional upper layer(s) of organic matter on the mean annual ground temperatures. In the results section we illustrate the model outputs and provide the per decadal warming rates at

[2] Circumpolar Active Layer Monitoring Network http://www.udel.edu/Geography/calm/

TCD
6, 89–124, 2012

different depths during the 21st century. The discussion section gives an overview on major physical factors that affect permafrost thermal regime and outlines how the model can be improved. Finally, conclusion section outlines major results and concludes the current work.

1.1 An overview of permafrost modeling

In the past, one of the most popular methods in permafrost mapping was the use of a frost number or permafrost index methods (Nelson, 1986). Indexing methods usually take into account seasonal air temperature variations explicitly and do not include other important factors (snow, soil moisture content, soil thermo-physical parameters) that affect permafrost thermal state.

Riseborough et al. (2008) divide permafrost models into three main categories: empirical, equilibrium and numerical. Empirical models relate permafrost occurrences to topoclimatic factors and use empirically derived landscape parameters representing the response of the active layer and permafrost to both climatic forcing and local factors, such as soil properties, moisture conditions and vegetation (Nelson et al. 1997; Shiklomanov and Nelson 2002; Zhang et al. 2005; Shiklomanov et al. 2008). Equilibrium models use so called transfer functions between the air and ground temperatures to define the active layer depth. The Kudryavtsev Model, N factor, TTOP and GIPL 1.0 models are classified as equilibrium models (Kudryavtsev et al. 1974; Romanovsky and Osterkamp 1995; Romanovsky and Osterkamp 1997; Shiklomanov and Nelson 1999; Klene et al. 2003; Sazonova and Romanovsky 2003; Wright et al. 2003.). However, applicability of equilibrium models is restricted to problems of limited complexity, and where the transient effects may be neglected or unimportant. Numerical solution methods are generally used to solve freezing and thawing problems over a short (engineering) time scale, where the transient effects of phase change are important (see Williams and Smith, 1989, pg. 86). Therefore, transient numerical modeling (e.g., Gruber et al., 2004a,b; Nicolsky et al., 2007; Farbrot et al., 2007; Etzelmuller et al., 2008) with incorporated phase change effect is the most effective method to simulate and forecast the thermal regime of permafrost over a relatively short time interval. The transient numerical model takes longer to run calculations. The pay off in this case is a more accurate determination of the temperature field and phase change boundary dynamics.

2 Mathematical model

The GIPL2-MPI numerical model solves the Stefan problem with phase change which is the problem of thawing or freezing via conduction of heat. Tracking a moving phase change boundary is the main difficulty in solving the Stefan problem. The enthalpy formulation is used in the solution of Stefan problem in GIPL2-MPI model, which is one of the common methods that does not require explicit treatment of the moving boundary (Caldwell and Chan, 2001).

The core of the GIPL2-MPI numerical model is based on the 1-D quasi-linear heat conductive equation (Sergueev et al., 2003):

$$\frac{\partial H(x,t)}{\partial \tau} = \mathrm{div}(k(x,t)\nabla t(x,\tau)) \tag{1}$$

where $x \in (x_u, x_l)$ is a spatial variable which changes with depth and $\tau \in (0, T]$ is a temporal variable. $k(x,t)$ is thermal conductivity ($\mathrm{Wm^{-1}K^{-1}}$); $H(x,t)$ is an enthalpy function.

$$H(x,t) = \int_0^t C(x,s)ds + L\Theta(x,t) \tag{2}$$

where $C(x,s)$ is volumetric heat capacity ($\mathrm{MJm^{-3}K^{-1}}$), and $\Theta(x,t)$ is volumetric unfrozen water content (%); L is the volumetric latent heat of freeze/thaw ($\mathrm{MJm^{-3}}$). The equation (1) is complemented with boundary and initial conditions. The upper part

TCD
6, 89–124, 2012

of the domain corresponds to the air layer which is at two meters height above the surface. The fictitious domain formulation (Marchuk et al., 1986) allows to embed seasonal snow layer into the current air layer. The Dirichlet type boundary condition was used as an upper boundary condition

$$t(x_u,\tau) = t_{\text{air}} \tag{3}$$

where t_{air} is a monthly averaged air temperature. The geothermal gradient was set at the lower boundary:

$$\frac{\partial t(x_l,\tau)}{\partial x} = g \tag{4}$$

where g is geothermal gradient, a some small constant number (Km^{-1}). For initial temperature distribution we used an appropriate ground temperature profile based on the point location

$$t(x,0) = t_0(x). \tag{5}$$

The formula for unfrozen water content $\Theta(x,t)$ is based on empirical experiments and has the following form:

$$\Theta(x,t) = \eta(x) \cdot \begin{cases} 1, & t \geq t_* \\ a|t|^{-b}, & t < t_*. \end{cases} \tag{6}$$

Parameters a and b are dimensionless positive constants (Lovell, 1957), $\eta(x)$ is a volumetric soil moisture content. The constant t_* is a freezing point depression, which from a physical point of view means that ice doesn't exist in the soil if $t > t_*$. $\Theta(x,t)$ changes with depth and depends on the soil type. The discritized form of the equation (1) can be found in Sergueev et al. (2003) and Marchenko et al. (2008). A detailed mathematical description of the model and numerical solution methods can be found in Nicolsky et al. (2007).

TCD
6, 89–124, 2012

3 Methods

We implemented the Scenarios Network for Alaska Planning (SNAP) dataset as a baseline input for the GIPL2-MPI numerical model. The dataset is composed of five GCMs which according to SNAP, performed the best for Alaska. It includes monthly averaged temperature and precipitation data for the years 1980–2099. The output from the selected five models were downscaled to 2 by 2 km resolution by SNAP using the knowledge-based system PRISM [3]. PRISM uses a digital elevation model that contains information describing Alaska's topography (slopes, aspects, elevations) and observed precipitation measurements to determine variations in precipitation as functions of elevations.

To calculate snow depth and its thermal conductivity we developed the following method outlined below. Snow density is calculated according to (Verseghy, 1991):

$$\rho_0 = \rho_{\mathrm{smin}}, \quad \rho_i = (\rho_{i-1} - \rho_{\mathrm{smax}})e^{-\tau_f \Delta\tau} + \rho_{\mathrm{smax}}. \tag{7}$$

where $\tau_f = 0.24$ corresponds to an e-folding time of about 4 days, ρ_s is the snow density in unit of $\mathrm{kg \cdot m^{-3}}$, and the value of ρ_s ranges from minimum snow density ρ_{smin} to maximum snow density ρ_{smax}, with a time step $\Delta\tau$ of one month. We chose ρ_{smin} and ρ_{smax} from the corresponding snow class following (Sturm et al., 1995). Snow depth h_s is calculated by extracting snow water equivalent (SWE) from the downscaled five GCM composite precipitation dataset.

$$h_s = \frac{\mathrm{SWE}}{\rho_s} \tag{8}$$

Snow thermal conductivity k_s was calculated according to (Sturm et al., 1997).

$$k_s = 0.138 - 1.01\rho_s + 3.233\rho_s^2. \tag{9}$$

[3]Parameter-elevation Regressions on Independent Slopes Model climate mapping system (http://www.prism.oregonstate.edu)

TCD
6, 89–124, 2012

Snow water equivalent was extracted from the precipitation dataset by comparing monthly mean temperatures (MMT) with the water freezing point temperature. If the MMT is less than the 0°C then we accumulate the SWE on monthly basis (i.e. since snow stays on the ground after first time fall we add existed SWE to the SWE for the current month). When the SWE is obtained, we calculate density, depth and thermal conductivity of the snow by employing equations (7)–(9).

Initial distributions of temperature with respect to depth were derived from the borehole temperature measurements obtained in Alaska by different researchers during the last several decades (Brewer 1958, Lachenbruch and Marshall 1986, Osterkamp and Romanovsky 1999, Clow and Urban 2002). Based on similar patterns of ground temperatures profiles for a specific geographic location, we classify initial temperature distribution profiles into eighteen geothermal zones (Fig. 1).

For the top soil layers, we used the data obtained from geophysical surveys and from the National Atlas of the United States of America [4]. Thermal properties of mineral soils were prescribed based on the Modified Surficial Geology Map of Alaska (Karlstrom , 1964). We assigned multilayered thermal parameters according to the lithological structure of a specific area and classified thermal properties into twenty-six different classes.

The active layer thickness (ALT) in the model is calculated according to the unfrozen water function (6) and unfrozen water saturation coefficient (UWSC). The UWSC is equal to 95 % and serves as a threshold between frozen and thawed state (i.e. freeze/thaw moving front correspond to state when the degree of soil layer saturation passes UWSC). The ALT correspond to the deepest upper freeze/thaw front over the hydrological year cycle.

Each grid point on the map uses a one-dimensional multi-layer soil profile down to the depth of 700 m. The vertical grid has fine resolution between nearby points at the near surface ground layer (0.01 m) and gets more coarser towards the bottom boundary (100 m). The geothermal heat flux is assigned as a lower boundary condition. The

[4] http://www.nationalatlas.gov

TCD
6, 89–124, 2012

values for the geothermal heat flux were generated using Pollack's geothermal heat model (Pollack et al., 1993).

4 Model calibration and validation

For initial model calibration we used measured data from more than fifteen shallow boreholes (1–1.2 m in depth) across Alaska. These ground temperature measurements are of a very high quality (precision generally at 0.01 °C) and available for the period from the mid-1990 to 2010. At most of these boreholes, measurements of soil water content and snow depth are also available. Figures 2 through 4 illustrate the results of the model calibration for the three shallow borehole stations. The West Dock site is located on the outer Arctic Coastal Plain within the Prudhoe Bay oil field. The polygonized "uplands" and drained thaw-lake basins constitute the primary relief at this site. Landcover units include Graminoid-moss tundra (wet nonacidic). The site were described by Osterkamp (1987) and Romanovsky and Osterkamp (1995). The Sag-Mat site is located on a north facing slope of about 2 degrees. The vegetation cover is a moist acidic tundra (Walker et al., 2008). Galibraith Lake site is located in previously glaciated mountain valley. Landcover units include graminoid-moss tundra and graminoid, prostrate-dwarf-shrub, moss tundra (wet and moist nonacidic). Further site description can be found in Ping et al. (2003). All these sites were instrumented by at least ten thermistors arranged vertically at depths from 0m to 1 m. The detailed description on thermistors set up and installation can be found in Nicolsky et al. (2007). For all compared stations correlation between GCMs and observations is higher than 90 % for monthly mean air temperatures (MMAT). Despite the high correlation between downscaled and observed MMATs the freezing and thawing periods are not always well satisfied with the downscaled GCMs composite. As it can be seen from Fig. 2 the variances between simulated and measured ground temperatures during 1999 freezing period increase with depth. Simulated monthly averaged ground temperatures drops more sharply forced by the MMAT when the actual ground temperatures

TCD
6, 89–124, 2012

Numerical modeling of permafrost dynamics in Alaska

E. E. Jafarov

freezing period is longer. The same pattern can be observed during thawing period (e.g. SagMat thawing period 2004–2005, Fig. 3). Moreover, there are winter periods when the actual monthly averaged ground temperatures are colder than simulated (see SagMat thawing period 2002, 2004, 2005, Fig. 3, Galibraith Lake winter periods 2004, 2005, Fig. 4), which can be due to mismatches in snow conductivities and snow depths over those winter periods. Clearly, simulated temperatures are more smooth comparatively to measured and do not account for the seasonal effects which create the high variabilities when the two ground temperature profiles are compared.

To validate the model results we used annually averaged temperatures at deeper depths. More than 50 deep boreholes from 29 m to 89 m in depth (GTN-P [5]) were available for the model calibration in terms of permafrost temperature profiles. Figure 5 illustrates how well the measured and simulated mean annual ground temperatures match with observed data. For the most of the stations the deviation between observed and measured mean annual ground temperatures (MAGT) is less than 1 °C (Fig. 5). There are four stations where the deviation is higher than 1 °C, three of them are located in the tussock area. The tussock is consist of small hillock of grassy, or grass-like plant growth. The MAGTs for these areas are sensitive to the mean annual snow fall. If snow depth do not exceed the height of a tussock then tussocks allow cold air pernetrate deep to the ground, otherwise, when snow depth exceed the height of a tussock its isolates the ground from the cold air.The permafrost observation station with the measured −3.81 °C and simulated −6.32 °C MAGTs at depth 20 m correspond to the site in the continuous permafrost zone with MAAT around −10 °C. The fact that measured MAGT is almost 3 degrees warmer might be due to the site location which is around small lakes. The convective heat transfer due to ground water movements or heat from the open water reservoirs might be essential factors producing warmer MAGT.

[5]Global Terrestrial Network for Permafrost http://www.gtnp.org/

In addition to deep borehole stations we validate the model against the permafrost observation stations from US Schools project [6]. The measurements from these stations are taking at relatively shallow depths ranging from 1 to 6 m. Most of the stations are located in close proximities to public schools, rivers or lakes. There are three points with difference between measured and simulated temperatures larger than 3 °C. One of them located in Anchorage, another in Chevak village close to the lake and other one in Circle close to the one of the branches of Yukon river. The permafrost station in Anchorage is experiencing the influence of the anthropogenic warming. At the other two sites, in addition to the anthropogenic factor, the subsurface ground water movements might also contribute to the MAGT formation process.

Finally, we validate the simulated active layer thickness values with observed ALT values from 43 CALM [7] active layer observation stations in Alaska (Fig. 7). For ALT comparison test we compared measured averaged active layer thicknesses over available time period with corresponding model simulated ALTs. During ALTs simulation the soil moisture content is specified for each of the simulated station and held constant throughout the entire simulation period. The major restriction of this approach reflects the limitation of available data on soil moisture content and its dynamics over time for each of the compared stations. There are two main uncertainties, while comparing simulated and measured ALT. The first one comes form the active layer measuring method. There are several methods on measuring ALT all of them has their own limitations (Nelson and Hinkel, 2003). The second uncertainty comes from the simulated AL depth, which is driven by monthly averaged climate data and by the amount of prescribed soil moisture content. During model validation against the MAGT datasets as well as ALT against CALM stations the values for several observation stations have been adjusted by assigning additional organic layers.

[6]IPA-IPY Thermal State of Permafrost (TSP) Snapshot Borehole Inventory, Version 1.0 (http://nsidc.org/data/g02190.html)

[7]Circumpolar Active Layer Monitoring Network http://www.udel.edu/Geography/calm/

TCD
6, 89–124, 2012

To evaluate the measure of the overall model performance and the model bias, we calculated the mean absolute error, root mean square error and mean bias error according to the following series of equations (Willmott and Matsuura, 2005):

$$\mathrm{MAE} = \frac{1}{n}\sum_{k=1}^{n}|e_i|, \quad \mathrm{RMSE} = \frac{1}{n}\sqrt{\sum_{k=1}^{n}e_i^2}, \quad \mathrm{MBE} = \frac{1}{n}\sum_{k=1}^{n}e_i. \tag{10}$$

where e_i is a difference between simulated and observed MAGTs and ALTs and n is number of stations. The MAE shows an overall error for all compared stations, when the RMSE emphasize an error variation within the individual stations. The negative values of MBE (Table 1) represent the model undestimation of the observed temperatures.

5 Model sensitivity analysis

Moderate MAAT and high variability of precipitation in western and southwestern parts of Alaska cause warmer MAGTs at 1 m depth after 30 years model run over some areas in the region. However, according to permafrost observation stations in those regions the MAGTs by the year 2010 at 1 m depth stay close to °C. These parts of Alaska correspond to subarctic oceanic and continental sub-arctic climate. During spring, when the Bering Sea is ice free the moderating influence of the open water helps to melt the snow early for some areas adjacent to the sea, when winter temperatures are more continental due to presence of sea ice (Serreze and Barry, 2005).The mean annual average of air temperatures is in a range from −1 °C to 2 °C from west to south-west of Alaska. These areas correspond to ecosystem protected permafrost zones that has formed under colder climate conditions and currently persist only in undisturbed late-successional ecosystems (Shur and Jorgenson, 2007). The MAGTs for the areas with sufficient amount of organic cover and soil moisture content usually experience gradual increase even when MAATs are slightly higher than 0 °C (Jorgenson et al., 2010). Apparently, assigned in the model soil organic layer thickenss does not provide enough

TCD
6, 89–124, 2012

insulation and causes warmer MAGTs at 1m depth after thirty years of calculation. Therefore, in order to provide permafrost resilience, an additional layer of organic matter is necessary. However, high variability of precipitation and thermal properties of mineral soils at a specific grid point make the choice of the appropriate organic layer non-trivial.

To address this problem we developed an algorithm, which assigns optimal additional organic layer for each grid point based on deviation coefficient of the equilibrium temperature profile from its initial ground temperatures. During model calibration we test the effects of varying climatic and ecological conditions on ground temperatures and developed nine classes of the different additional organic layers. The additional organic layers varies from thinner to thicker and differs by the amount of soil moisture and have different thermo-physical properties.

The algorithm based on the following principle. If assigned initial temperature profile represent actual ground temperature distribution for the year 1980 then equilibrated ground temperatures should not deviate significantly from initial temperature distribution profile as it has been observed for these regions (Romanovsky et al., 2010; Smith et al., 2010). Otherwise, we assign additional organic layer for corresponding grid point in successive manner. The organic layer corresponding to the smallest deviation coefficient sets as a final additional organic matter.

The obtained additional organic layer mask (Fig. 8) excludes lakes, rivers and mountain areas and shows places where differences between initial temperature profiles and equilibrated temperature profile is significant. The places required additional organic layers (AOL) located mostly in discontinues permafrost zone. The amount of AOL in north western part is thin and not so extensive in comparison to southwestern territories. The thickness of the AOL is getting more diverse in south and southwest zones. The AOL mask indicates the places where the initial temperature profiles should be adjusted. As it was mentioned in methods section the initial temperature profiles were assigned according to the measured data, which are available for limited number of places and does not cover the entire region.

TCD
6, 89–124, 2012

Figure 9 illustrates the model runs with and without AOL. The MAGTs according to results with AOL mask at 1m depth are slightly colder in western and southwestern parts which might more closely represent current ground temperature distribution. This sensitivity analysis indicates the significance of the appropriate organic layer presence in order to keep MAGT colder and provide permafrost with necessary resilience within the ecosystem-protected permafrost zone. This analysis also emphasized the importance of improved maps of soil organic layers and the necessity of further development of the permafrost temperatures observation system, especially in western and southwestern parts of Alaska.

6 Results

To ensure that the initial temperature conditions did not influence results we ran the spin up with assigned initial ground temperature profiles (Fig. 1) corresponding to the middle of the August 1980, until the soil temperature profile reached equilibrium with the upper and lower boundary conditions. The equilibrium temperature profile was determined when the maximum difference of soil temperatures at all levels between two successive time steps was less than 0.01 °C and used as the initial condition.

According to the decadal average of MAGTs histogram over twelve decades from 1980 to 2099 the overall area covered by MAGT less than 0 °C is going to decrease at different rates. The model projects the areal increase of the averaged decadal MAGT warmer than 0 °C at 2, 5 and 20 m depth with rates 3.7 %, 3.5 % and 2.4 % per decade correspondingly (Fig. 10).

The spatial snapshot of MAGTs at 2 m depth below the surface (Fig. 11) shows pronounced warming almost everywhere including currently continuous permafrost areas (e.g. Seward Peninsula and the South part of Brooks Range). As it was mentioned in sensitivity section the amount of ground surface organic material retards the permafrost thaw in the discontinuous permafrost zone. This effect can carried on to continues permafrost zone via changes in vegetation. Therefore, discontinues and sporadic permafrost areas with small or no organic layer on top and little soil moisture content will be more vulnerable to the rapid permafrost thaw. High altitude areas such as Chugach Mountains, Wrangell Mountains, Alaska and Brooks Range maintain relatively stable MAGTs during first half of the 21st century due to cold annual air temperatures.

The mean annual air temperature (MAAT) dynamics for 120 years from downscaled five GCMs composite showed larger positive temperature trend during the 21st century for the northern region. This high positive trend can be observed almost everywhere north from the Brooks Range. The simulated mean annual snow depth showed that the amount of annual snow fall decreases in the south and increases in the north, when the number of snow-free days increase in the whole region due to warmer MAATs. The increase of snow-free days and at the same time, the increase of the thickness of snow, which is an insulation layer, greatly affects the mean annual surface temperatures in Northern part of Alaska. Eventually, this effect propagates further to the ground and transfers to the MAGTs. The Fig. 12 illustrates the higher trend of the MAGT for the two northern sites in comparision with central and south-central locations.

7 Discussion

The GIPL2-MPI transient numerical model with proper input parameters is a valuable tool for mapping the thermal state of permafrost and its future dynamics with high spatial resolution. However, it is important to understand the limitations of the current model and the downscaled GCMs composite dataset.

The composite of five downscaled GCMs simulate well the seasonal cycle variations of near-surface temperature with correlation between models and observations of 90 % or higher (Fig. 2–4). However, the bias in climate model simulation of precipitation still remains high, correlation between GCMs and observations is 50 to 60 % (Bader et al., 2008).

TCD
6, 89–124, 2012

The stations where GIPL2-MPI model showed high discrepancies with observed MAGTs (Fig. 6) were established recently (2005–2009) and do not have long term data for more comprehensive analysis. The significant number of those stations located along the rivers and in populated areas. The high order differences between measured and simulated MAGT might be caused by changes in surficial geology (due to flooding), ground water movement (convective heat transfer) or anthropogenic disturbances.

Besides the described above factors affecting the permafrost ground temperatures simulations, there is also such an important factor as forest fires. As a result of the fires, the surface albedo decreases and the soil thermal conductivity of the surface soil layer increases (Hinzman et al., 1991). The areas where wildfires removed the upper organic layer are vulnerable to the active layer increasing in depth and warming of permafrost. If the burned area is ice reach then the increase of active layer might melt the buried ice, which would cause the soil to collapse and form thermokarst depressions (Yoshikawa et al., 2002). In order to address the dynamics of the mean annual ground temperatures of the burned area it is important to include in the model the dynamics of the corresponding vegetation and organic layers development after the fire event. At the current stage the model does not include the effect of forest fires.

The MAGTs in continuous permafrost zone are mostly climate-driven, when for the discontinuous permafrost zone the effect of the ecosystem on the permafrost thermal state is more pronounced (Shur and Jorgenson, 2007). With climate warming present day continuous permafrost will turn into discontinuous and vegetation change can develop enough upper organic layer which will provide permafrost with additional resilience to thaw. Therefore introduction of the dynamic vegetation layer might decrease current modeling bias for discontinues permafrost zone. In the GIPL2-MPI spatial model the ecosystem effect can be addressed via surface organic layer, soil moisture content and thermo-physical properties of the soils. To better quantify the ecosystem effect in discontinuous permafrost zone further sensitivity analysis on the impact of each of the influencing factors as well as the combination of several factors based on specific geographic location and climatic zone is necessary. The impact of humans and wildfires have to be taken into consideration where it is necessary. Further work is needed to improve parametrization of soil properties for each type of surface and soil conditions. Development of the spatial soil moisture map for Alaska region will improve understanding of the soil moisture distribution and its dynamics as well as the results of permafrost modeling. Methods for calculating snow depth and snow thermal properties require further improvement. The 2km distance between adjacent points is far enough to neglect lateral heat transfer. However, for the grid resolution finer than 1km this assumption might not hold true, due to convective heat transfer by ground water movement. Therefore, coupling the current model with a hydrological model would be an important step towards better simulation results for watershed and wetland areas.

8 Conclusions

The increase in mean annual air temperatures and in amount of precipitation for the northern part of the region predicted by five GCM composite with A1B emission scenario could accelerate permafrost warming in the North (Fig. 12). Depending on the corresponding ecosystem type, the central part of the region would experience permafrost degradation at different severity levels. The effect of the upper organic layer, soil water saturation, and soil thermal properties play a significant role and provide necessary resilience for permafrost to sustain even when MAAT are close or slightly above 0 °C. To provide an estimate of the permafrost degradation severity level for a specific geographic location the effects of varying climatic and ecological conditions require more detailed investigation and may require modeling with even higher spatial resolution.

According to the modeling results average areal decadal permafrost degradation at 20 m depth can be pursued with 2.4 % rate per decade, which concludes that for the next 90 years Alaska could lose about 22 % of its currently frozen ground. Further analysis and development of the model is required to improve the MAGTs and

ALTs simulations. In order to cover more accurately the entire region and to decrease uncertainty in the model predictions more permafrost temperature observation stations are necessary. The increase in the grid spatial resolution requires high resolution maps of surficial geology, precipitation, vegetation, surface organic layer and soil moisture content.

Acknowledgements. We would like to thank the friendly personal at ARSC Supercomputing Center. In particular Tom Logan and Don Bahl for their help with code parallelization and constant assistance on model performance and Kate Hedstrom and Patrick Webb for their help with visualization software. Especial thanks to Kenji Yoshikawa for the data from high school project. We also would like to thank CSDMS staff for letting us to run the model on the beach HPCC. This work was supported by the National Science Foundation under grants ARC-0520578, ARC-0632400, ARC-0856864, ECOMODI and the State of Alaska.

References

Bader, D. C., Covey, C., Gutowski, W. J. J., Held, I. M., Kunkel, K. E., Miller, R. L., Tokmakian, R. T., and Zhang, M. H.: Climate Models: An Assessment of Strengths and Limitations, Tech. rep., US Climate Change Science Program and the Subcommittee on Global Change Research, Department of Energy, Office of Biological and Environmental Research, Washington, D.C., USA, 2008. 104

Brewer, M. C.: Some Results of Geothermal Investigations of Permafrost in Northern Alaska, Transaction, AGU, 39, 19–26, 1958. 97

Brown, J., Smith, S. L., Romanovsky, V., Christiansen, H. H., Clow, G., and Nelson, F. E.: In Terrestrial Essential Climate Variables for Assessment, Mitigation and Adaptation, WMO Global Climate Observing System report GTOS-52, 24–25, 2008. 91

Caldwell, J. and Chan, C. C.: Numerical solution of Stefan problems in annuli by enthalpy method and heat balance integral method, Numer. Methods Eng, 17, 395–405, 2001. 94

Clow, G. D. and Urban, F. E.: Largest permafrost warming in northern Alaska during the 1990s determined from GTN-P borehole temperature measurements, EOS, Transactions of the AGU, 83, F258, 2002. 97

Etzelmuller, B., Schuler, T. V., Farbrot, H., and Gudmundsson, A.: Permafrost in Iceland – distribution, ground temperatures and climate change impact., In Proceedings of the Ninth International Conference on Permafrost, 29 June–3 July 2008, 2008. 93

Farbrot, H., Etzelmüller, B., Schuler, T. V., Gudmundsson, Á., Eiken, T., Humlum, O., and Björnsson, H.: Thermal characteristics and impact of climate change on mountain permafrost in Iceland, J. Geophys. Res., 112, F03S90, doi:10.1029/2006JF000541, 2007. 93

Gruber, S., Hoelzle, M., and Haeberli, W.: Permafrost thaw and destabilization of Alpine rock walls in the hot summer of 2003., Geophys. Res. Lett., 31, 4 pp., doi:10.1029/2006JF000547, 2004a. 93

Gruber, S., Hoelzle, M., and Haeberli, W.: Rock-wall temperatures in the alps: modeling their topographic distribution and regional differences., Permafrost Periglacial Processes, 15, 299–307, doi:10.1002/ppp.501, 2004b. 93

Hinzman, L. D., Kane, D. L., Gieck, R. E., and Everett, K. R.: Hydrologic and thermal properties of the active layer in the Alaskan Arctic, Cold Reg. Sci. Technol., 19, 95–110, 1991. 105

Jorgenson, M. T., Romanovsky, V., Harden, J., Shur, Y., O'Donnell, J., Schuur, E. A. G., Kanevskiy, M., and Marchenko, S.: Resilience and vulnerability of permafrost to climate change, Can. J. Forest Res., 40, 1219–1236, doi:10.1139/X10-060, http://dx.doi.org/10.1139/X10-060, 2010. 101

Karlstrom, T. N. V.: Surficial Geology of Alaska, U.S. Geol. Surv., Misc. Geol. Inv. Map I-357, scale 1:1,584,000, 1964. 97

Klene, A. E., Hinkel, K. M., and Nelson, F. E.: The Barrow Urban Heat Island Study: Soil temperatures and active-layer thickness, in: in Proceedings of the Eighth International Conference on Permafrost, edited by: Balkema, L. A., 1, 555–560, Phillips M, Springman SM, and Arenson LU, 2003. 93

Kudryavtsev, V. A., Garagula, L. S., Kondratyeva, K. A., and Melamed, V. G.: Osnovy merzlotnogo prognoza , MGU, 431 pp., 1974 (in Russian).[CRREL Translation: V. A. Kudryavtsev et al., Fundamentals of Frost Forecasting in Geological Engineering Investigations, CRREL Draft Translation 606, 1977, 489 pp.] 93

Lachenbruch, A. H. and Marshall, B. V.: Changing climate: Geothermal evidence from permafrost in the Alaskan Arctic, Science, 234, 689–696, 1986. 97

Larsen, P. H., Goldsmith, S., Smith, O., Wilson, M. L., Strzepek, K., Chinowsky, P., and Saylor, B.: Estimating future costs for Alaska public infrastructure at risk from climate change, Global Environmental Change, 18, 442–457, 2008. 91

Lovell, C.: Temperature effects on phase composition and strength of partially frozen soil, Highway Research Board Bulletin, 168, 74–95, 1957. 95

Marchenko, S., Romanovsky, V., and Tipenko, G.: Numerical modeling of spatial permafrost dynamics in Alaska, in: In Proceedings of the Eighth International Conference on Permafrost, 190–204, Willey, Institute of Northern Engineering, University of Alaska, Fairbanks, 2008. 91, 95

Marchuk, G. I., Kuznetsov, Y. A., and Matsokin, A. M.: Fictitious domain and domain decomposition methods, Soviet J. Num. Anal. Math. Modelling, 1, 1–86, 1986. 95

Nelson, F. E.: Permafrost Distribution in Central Canada: Application of a Climate-Based Predictive Model, Annals of the Association of American Geographeers, 76, 550–569, 1986. 93

Nelson, F. E. and Hinkel, K. M.: Methods for measuring active-layer thickness, in: A Handbook on Periglacial Field Methods, edited by: Humlum, O. and Matsuoka, N., available online: http://www.udel.edu/Geography/calm/research/measurements.html, 2003. 100

Nelson, F. E., Shiklomanov, N. I., Mueller, G. R., Hinkel, K. M., Walker, D. A., and Bockheim, J. G.: Estimating active layer thickness over a large region: Kuparuk River Basin, Alaska, USA, Arctic and Alpine Research, 19, 367–378 24, 1997. 93

Nicolsky, D. J., Romanovsky, V. E., and Tipenko, G. S.: Using in-situ temperature measurements to estimate saturated soil thermal properties by solving a sequence of optimization problems, The Cryosphere, 1, 41–58, doi:10.5194/tc-1-41-2007, 2007. 93, 95, 98

Osterkamp, T.: Freezing and Thawing of Soils and Permafrost Containing Unfrozen Water or Brine, Water Resour. Res., 23, 2279–2285, 1987. 98

Osterkamp, T. and Romanovsky, V.: Evidence for Warming and Thawing of Discontinuous Permafrost in Alaska, Permafrost and Periglacial Processes, 10, 17–37, 1999. 97

Ping, C. L., Michaelson, G. J., Overduin, P. P., and Stiles, C. A.: Morphogenesis of frost boils in the Galbraith Lake area, Arctic Alaska, Proceedings of the Eighth International Conference on Permafrost, Zürich, Switzerland., 897–900, 2003. 98

Pollack, H. N., Hurter, S. J., and Johnson, J. R.: Heat Flow from the Earth's Interior: Analysis of the Global Data Set, Rev. Geophys., 31, 267–280, 1993. 98

Richter-Menge, J. and Jeffries, M.: The Arctic [in "State of the Climate in 2010"], Bull. Amer. Meteor. Soc., 92, 143–160, 2011. 91

Riseborough, D., Shiklomanov, N., Etzelmuller, B., Gruber, S., and Marchenko, S.: Recent advances in permafrost modeling, Permafrost and Periglacial Processes, 19, 137–156, optional, 2008. 93

Romanovsky, V. and Osterkamp, T.: Interannual variations of the thermal regime of the active layer and near-surface permafrost in Northern Alaska, Permafrost Periglac., 6, 313–335,

1995. 93, 98
Romanovsky, V. and Osterkamp, T.: Thawing of the active layer on the coastal plain of the alaskan arctic, Permafrost Periglac., 8, 1–22, 1997. 93
Romanovsky, V. E., Smith, S. L., and Christiansen, H. H.: Permafrost thermal state in the polar Northern Hemisphere during the international polar year 2007–2009: a synthesis, Permafrost Periglac., 21, 106–116, 2010. 91, 102
Sazonova, T. and Romanovsky, V.: A Model for Regional-Scale Estimation of Temporal and Spatial Variability of the Active Layer Thickness and Mean Annual Ground Temperatures, Permafrost Periglac., 14, 125–139, 2003. 93
Sergueev, D., Tipenko, G., Romanovsky, V., and Romanovskii, N.: Mountain permafrost thickness evolution under the influence of long-term climate fluctuations (results from numerical simulation), in: In 8th International Conference on Permafrost, edited by Swets & Zeitlinger: Lisse, Z., edited by: Phillips, M., Springmanm S., and Arenson, L., 1017–1021, 2003. 94, 95
Serreze, M. C. and Barry, R. G.: The Arctic Climate System, Cambridge University Press, http://dx.doi.org/10.1017/CBO9780511535888, 2005. 101
Shiklomanov, N. and Nelson, F.: Active-layer mapping at regional scales: A 13-year spatial time series for the Kuparuk region, north-central Alaska, Permafrost Periglac., 13, 219–230, doi:10.1002/ppp.425, 2002. 93
Shiklomanov, N., Nelson, F., Streletskiy, D., Hinkel, K., and Brown, J.: The Circumpolar Active Layer Monitoring (CALM) Program: Data collection, management, and dissemination strategies, in: In Proceedings of the Eighth International Conference on Permafrost, 210–217, Willey, Institute of Northern Engineering, University of Alaska, Fairbanks, 2008. 93
Shiklomanov, N. I. and Nelson, F. E.: Analytic representation of the active layer thickness field, Kuparuk River Basin, Alaska, Ecological Modeling, 123, 105–125, doi:10.1016/S0304-3800(99)00127-1, 1999. 93
Shur, Y. L. and Jorgenson, M. T.: Patterns of permafrost formation and degradation in relation to climate and ecosystems, Permafrost Periglac. Processes, 18, 7–19, doi:10.1002/ppp.582, http://dx.doi.org/10.1002/ppp.582, 2007. 101, 105
Smith, S., Romanovsky, V., Lewkowicz, A., Burn, C., Allard, M., Clow, G., Yoshikawa, K., and Throop, J.: Thermal state of permafrost in North America: a contribution to the international polar year, Permafrost Periglac., Fall Meet. Suppl., Abstract C12A-02, 21, 117–135, 2010. 91, 102
Sturm, M., Holmgren, J., and Liston, G. E.: A Seasonal Snow Cover Classification System for

Local to Global Applications, J. Climate, 8, 1261–1283, 1995. 96
Sturm, M., Holmgren, J., Konig, M., and Morris, K.: The thermal conductivity of seasonal snow, J. Glaciol., 43, 1997. 96
Tipenko, G., Marchenko, S., Romanovsky, V., Groshev, V., and Sazonova, T.: Spatially distributed model of permafrost dynamics in Alaska, EOS, Transactions of the AGU, 85(47), Fall Meet. Suppl., Abstract C12A-02, 2004. 91
Verseghy, D. L.: ClassA Canadian land surface scheme for GCMS. I. Soil model, International J. Climatol., 11, 111–133, doi:10.1002/joc.3370110202, http://dx.doi.org/10.1002/joc.3370110202, 1991. 96
Walker, D. A., Epstein, H. E., Romanovsky, V., Ping, C. L., Michaelson, G. J., Daanen, R., Shur, Y., Peterson, R. A., Krantz, W. B., Raynolds, M. K., Gould, W. A., Gonzalez, G., Nicolsky, D. J., Vonlanthen, C. M., Kade, A. N., Kuss, P., Kelley, A. M., Munger, C. A., Tamocai, C. T., Matveyeva, N. V., and Daniels, F. J. A.: Arctic patterned-ground ecosystems: A synthesis of field studies and models along a North American Arctic Transect, J. Geophys. Res.-Biogeo., 113, G03S01, 17 pp., 2008. 98
Williams, P. J. and Smith, M. W.: The Frozen Earth: Fundamentals of Geocryology, Cambridge University Press, 1989. 93
Willmott, C. J. and Matsuura, K.: Advantages of the mean absolute error (MAE) over the root mean square error (RMSE) in assessing average model performance, Clim. Res., 30, 79–82, http://www.int-res.com/abstracts/cr/v30/n1/p79-82/, 2005. 101
Wright, J. F., Duchesne, C., and Cote, M. M.: Regional-scale permafrost mapping using the TTOP ground temperature model, in: In Proceedings of the Eighth International Conference on Permafrost, edited by Balkema, L. A., 1241–1246, Phillips M, Springman SM, and Arenson LU, Zurich, Switzerland, 2003. 93
Yoshikawa, K., Bolton, W. R., Romanovsky, V. E., Fukuda, M., and Hinzman, L. D.: Impacts of wildfire on the permafrost in the boreal forests of Interior Alaska, J. Geophys. Res., 107, 8148, doi:10.1029/2001JD000438, 2002. 105
Zhang, T., Frauenfeld, O. W., Serreze, M. C., Etringer, A., Oelke, C., McCreight, J., Barry, R. G., Gilichinsky, D., Yang, D., Ye, H., Ling, F., and Chudinova, S.: Spatial and temporal variability in active layer thickness over the Russian Arctic drainage basin, J. Geophys. Res.-Atmos., 110, D16101, doi:10.1029/2004JD005642, 2005. 93

TCD
6, 89–124, 2012

Table 1. The model error statistics obtained by comparing MAGTs and ALTs from 3 different datasets: 60 deep borehole stations compared for 2007–2009 years; 77 US School project stations from relatively shallow depths compared for 2009; 43 averaged active layer thicknesses from CALM stations compared over entire available time periods.

Names	n	RMSE	MAE	MBE
Deep borehole stations (˚C)	60	0.70	0.59	−0.20
US School project (˚C)	77	0.88	1.23	−0.17
ALT (m) (CALM)	43	0.10	0.08	−0.02

TCD
6, 89–124, 2012

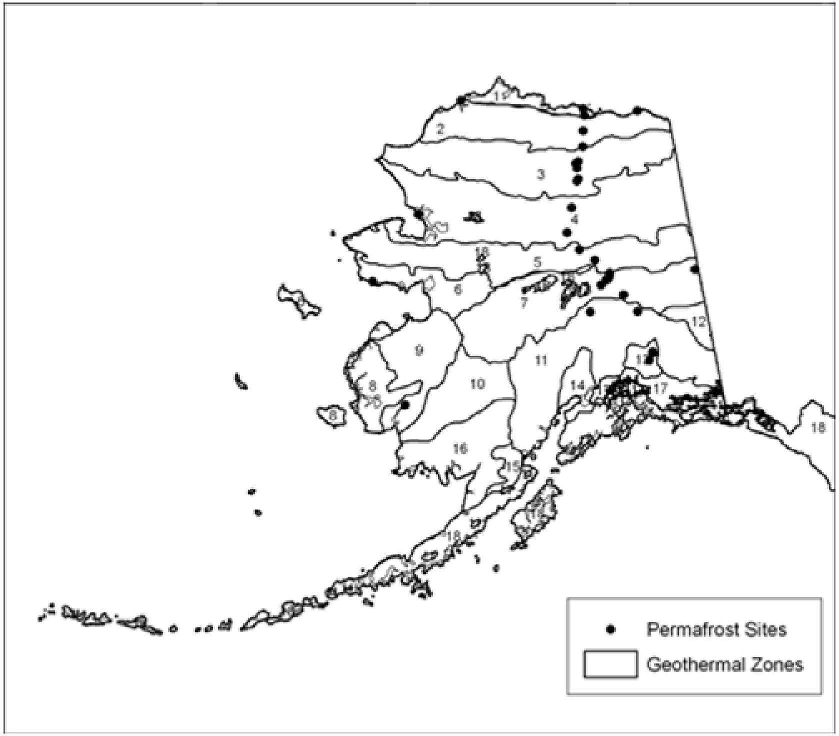

Fig. 1. Permafrost observation locations and geothermal zones. Each geothermal zone correspond to its own initial ground temperature distribution profile.

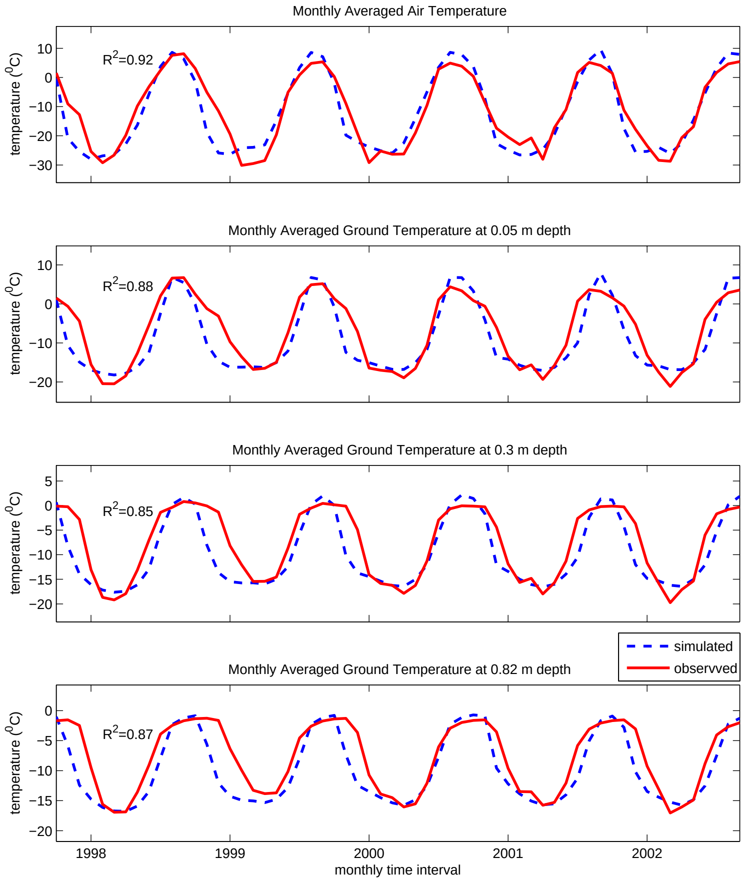

Fig. 2. Measured (solid) and calculated (dashed) monthly averaged temperatures at 2 m above the ground and 0.05, 0.3 and 0.82 m depth for WestDock 70.37° N, 148.55° W permafrost observation stations.

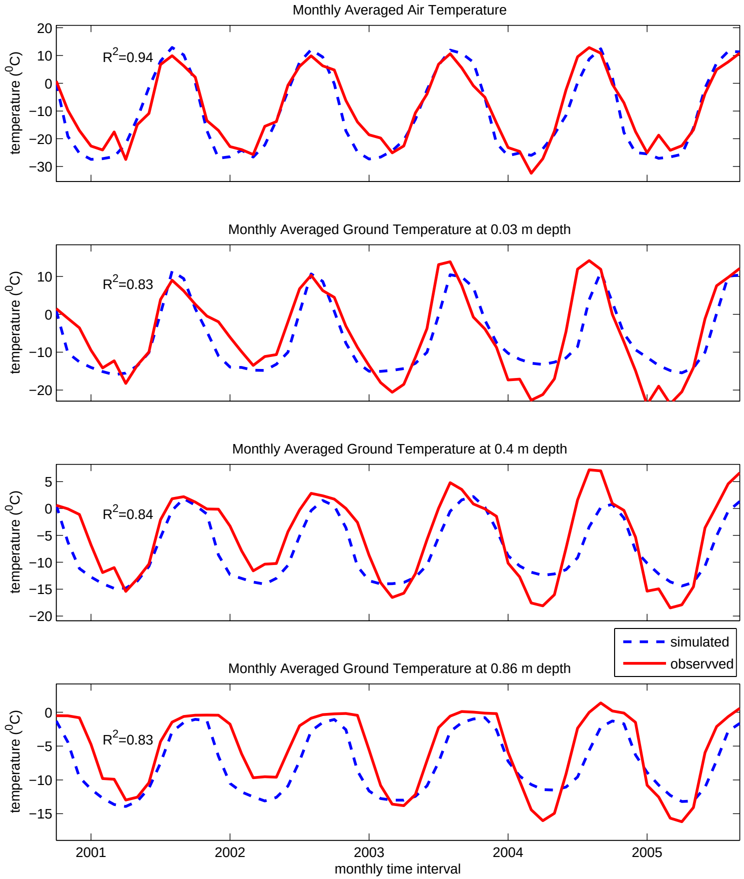

Fig. 3. Measured (solid) and calculated (dashed) monthly averaged temperatures at 2 m above the ground and 0.03, 0.4 and 0.86 m depth for SagMat 69.43° N, 148.70° W permafrost observation stations.

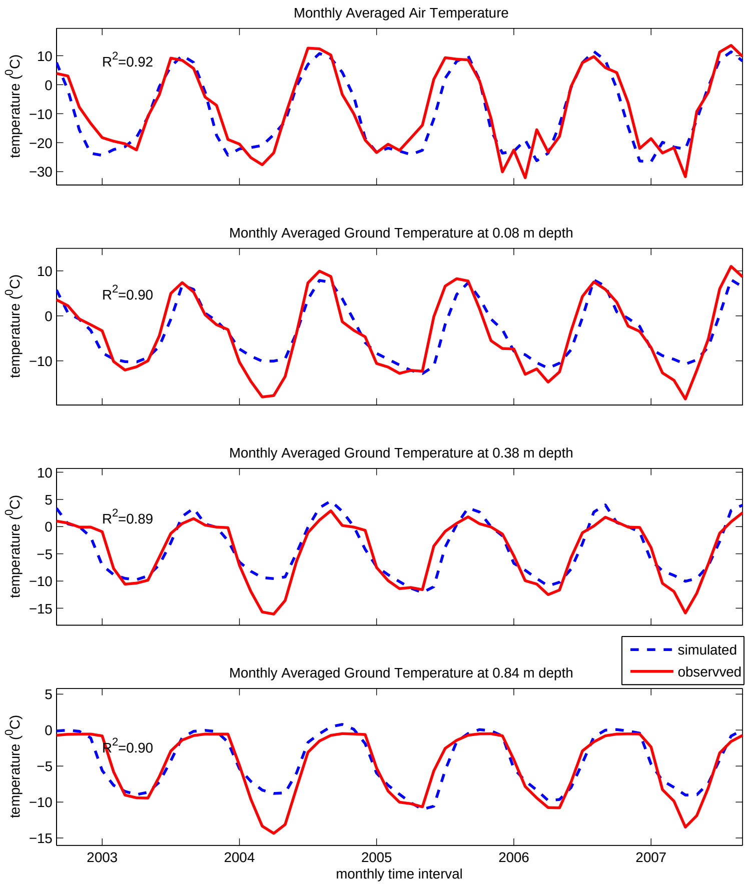

Fig. 4. Measured (solid) and calculated (dashed) monthly averaged temperatures atthe amount of saturated water coefficient 2 m above the ground and 0.08, 0.38 and 0.84 m depth for Galibraith Lake 68.48° N, 149.50° W permafrost observation stations.

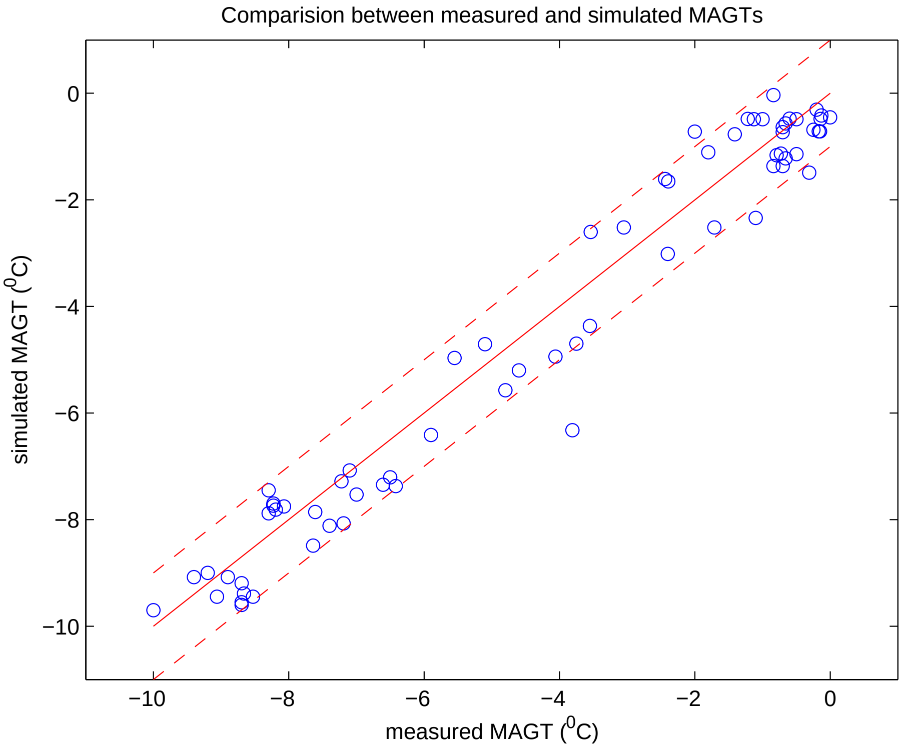

Fig. 5. Simulated and measured MAGTs at different depths from 3 to 30 m during 2007–2009 IPY years.

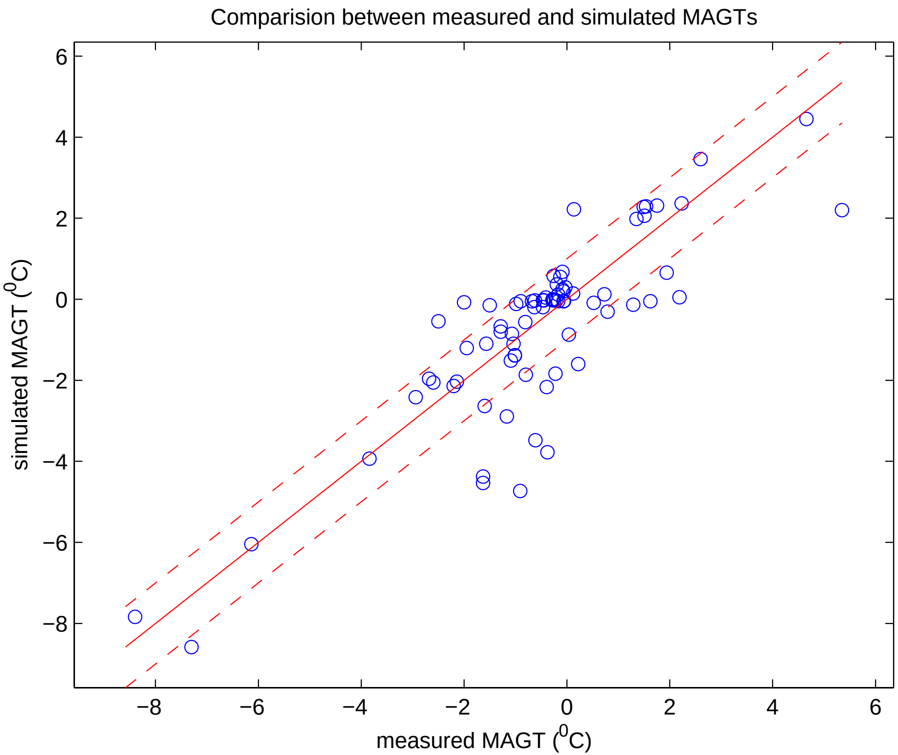

Fig. 6. Simulated and measured MAGTs from 1 to 6 m depths during 2009.

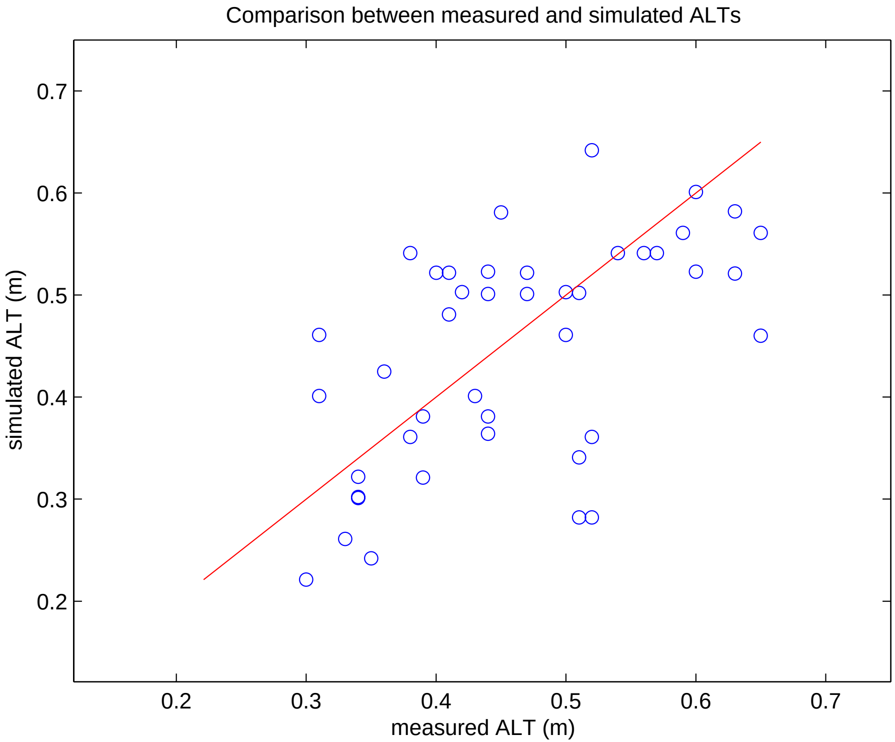

Fig. 7. Comparision between simulated and observed ALTs from 43 CALM observation stations.

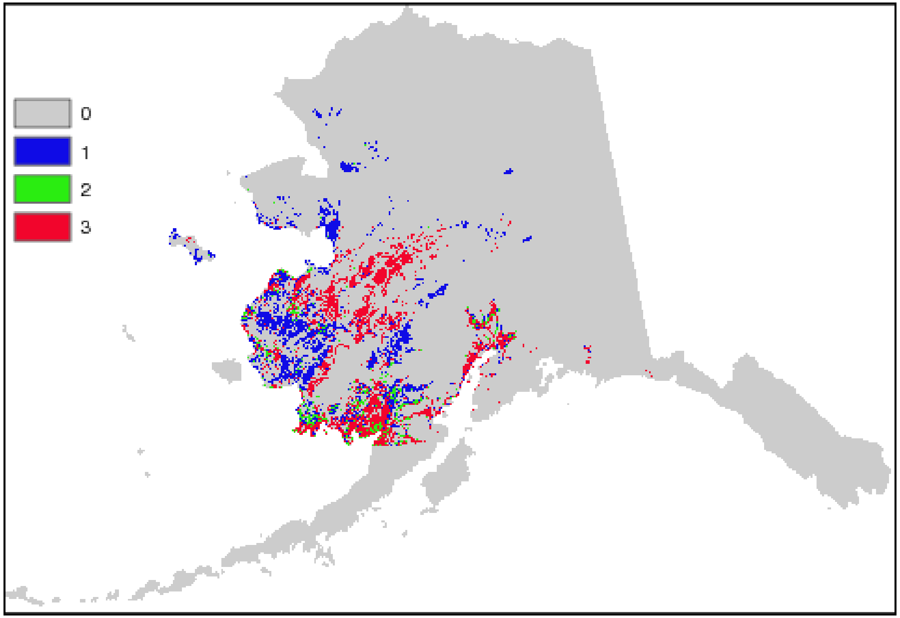

Fig. 8. Additional organic layer map obtained after model tuning. 0-no additional organic; 1-one additional layer of organic matter (5 cm); 2-two additional layers of organic matter (10 cm); 3-three additional layers of organic matter (27 cm).

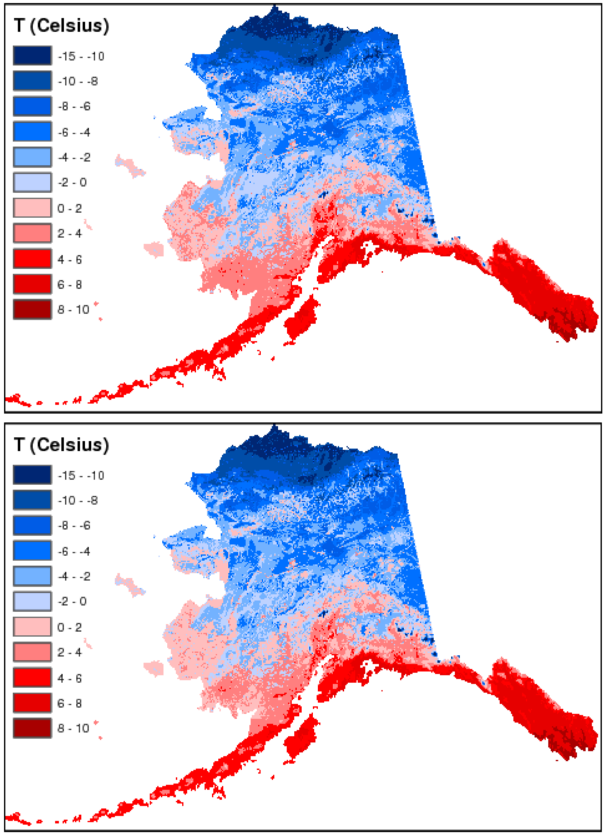

Fig. 9. Projected mean annual ground temperatures at 1 m depth for year 2010 **(a)** without and **(b)** with additional organic layer.

TCD

6, 89–124, 2012

Numerical modeling of permafrost dynamics in Alaska

E. E. Jafarov

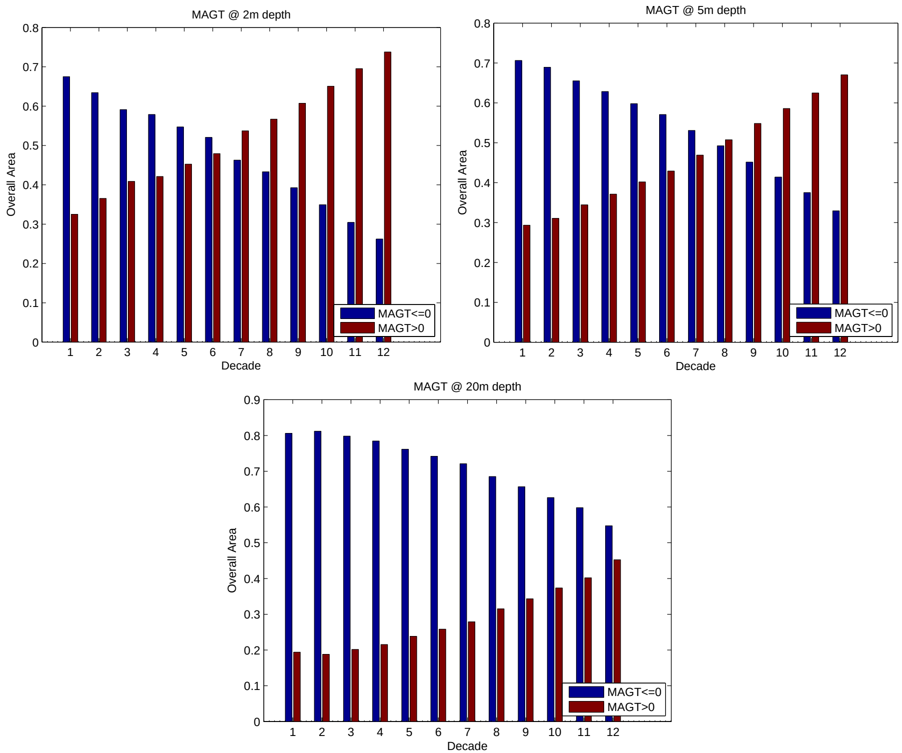

Fig. 10. The amount of area occupied by colder and warmer than 0 °C MAGTs averaged over ten years time interval from 1980 to 2099 at 2, 5 and 20 m ground depths.

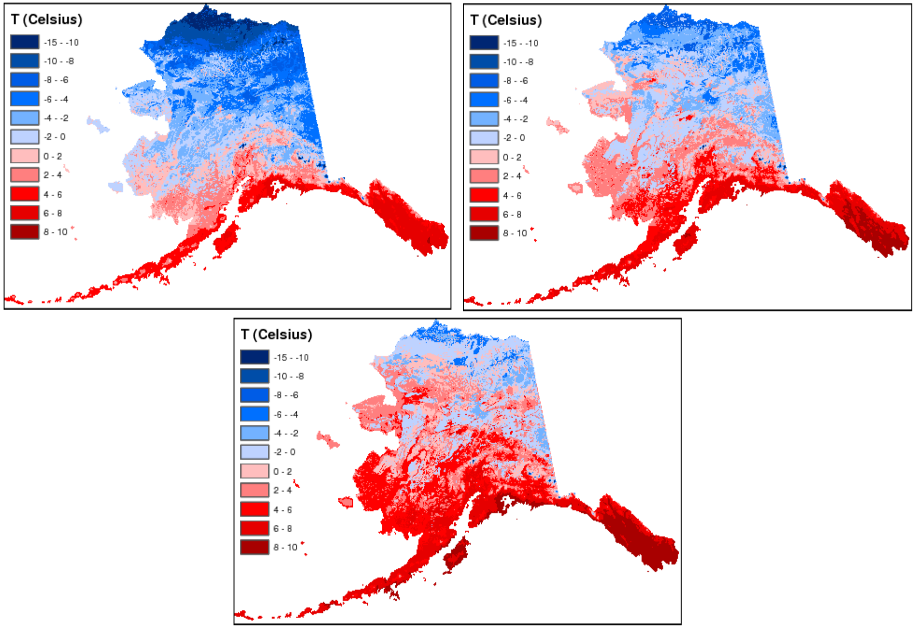

Fig. 11. Projected mean annual ground temperatures (MAGT) for the entire State of Alaska at 2 m depth using downscaled to 2 by 2 km climate forcing from GCM composite output with A1B emission scenario for the 21st century for years **(a)** 2000, **(b)** 2050 and **(c)** 2099.

TCD
6, 89–124, 2012

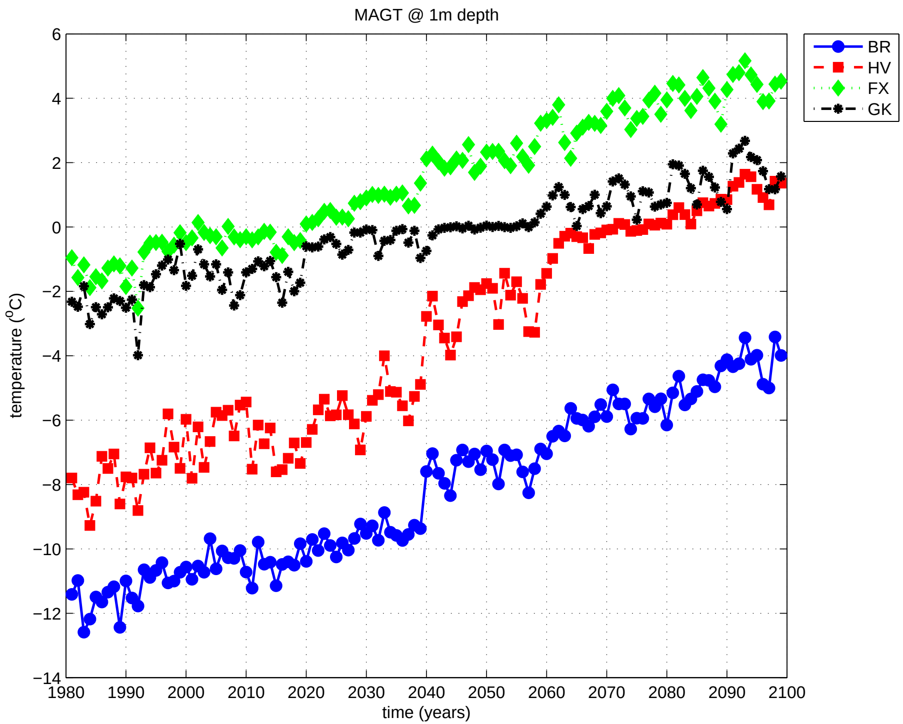

Fig. 12. Projected MAGT at 1 m depth for four different locations (Barrow, Happy Valley, Fairbanks, Gakona). Forcing from the downscaled five composite GCMs with A1B emission scenario.

TCD
6, 89–124, 2012